

short duration is such that a right switch following closely on an initial left break by E ceases to be effective. The pursuer of course initially runs directly toward the evader, and in this case E breaks to one side or the other when the separation is only slightly more than L . The subsequent composite motions end with E at E_2 , where his heading makes only about 10 deg with the sideline. E has gained about 10 yd compared with the final position E_1 . The diagram here indicates that the players are in contact at the tackle range over the majority of the time, as shown by the curved dashed lines.

Conclusions

Football is a multiplayer game analogous to the continental air defense problem. Real-space guidance constraints in such high-order games can be accounted for if the dynamics are simple, and differential-game mini-max optimization is feasible. Mathematical complexities occur if the evaders are faster than the pursuers.

References

- ¹Isaacs, R., *Differential Games—A Mathematical Theory of Warfare and Pursuit, Control and Optimization*, Wiley, New York, 1965, pp. 145, 231.
- ²Breakwell, J. V., "Pursuit of a Faster Evader," *Theory and Application of Differential Games; Proceedings of NATO Advanced Study Institute*, edited by J. D. Grote, Riedel, Dordrecht, The Netherlands, 1974, pp. 243–256.

Asymptotic Disturbance Rejection for Momentum Bias Spacecraft

Christopher D. Rahn*

Space Systems/Loral, Palo Alto, California 94303

Introduction

DURING the normal operation of momentum bias spacecraft, a control system maintains the pitch axis perpendicular to the orbit plane, the roll axis pointing along the orbital velocity vector, and the yaw axis pointing at the Earth's center. At least one momentum wheel spins to provide an angular momentum bias along the pitch axis.^{1–3} This pitch momentum is varied to control the pitch Euler angle of the spacecraft. Varying the wheel momentum along the yaw axis controls the roll and yaw Euler angles. An Earth sensor measures the roll and pitch angles. Yaw, though not directly measured, is observable from roll.

The accuracy to which the spacecraft maintains its prescribed attitude depends on the size and nature of the environmental disturbance torques. A previous technique⁴ improved pointing performance by estimating one component of these disturbance torques. This Note introduces a method of achieving asymptotic disturbance rejection through disturbance torque estimation and feedback. The method uses the Earth sensor roll signal, a full-order observer, a disturbance torque estimator, and magnetic torquers.

Roll/Yaw Dynamics

Dougherty et al.² determined the linearized equations of motion for a momentum bias spacecraft. They showed that the pitch dynamics are decoupled from the roll/yaw dynamics. Terasaki¹ derived the equations of motion for a system with yaw momentum storage. Lebsock⁴ assumed that the relatively

high-frequency roll/yaw nutation dynamics are damped by wheel control^{1,3–5} and neglected gravity gradient torques to generate the simplified momentum dynamics:

$$\dot{x} = Ax + Bu \quad (1)$$

with

$$a = \begin{bmatrix} H_x \\ H_z \end{bmatrix}, \quad A = \begin{bmatrix} 0 & \omega_o \\ -\omega_o & 0 \end{bmatrix}$$

$$B = \begin{bmatrix} 1 & 0 \\ 0 & 1 \end{bmatrix}, \quad u = \begin{bmatrix} M_x \\ M_z \end{bmatrix} \quad (2)$$

where H_x and H_z are the body axes roll and yaw angular momentum components, respectively; $\omega_o > 0$ is the orbit rate; and M_x and M_z are the body axes torques. The body axes torques equal the environmental disturbance torques T_{dx} and T_{dz} minus the magnetic control torques u_x and u_z ,

$$M_x = T_{dx} - u_x, \quad M_z = T_{dz} - u_z \quad (3)$$

The attitude errors, roll ϕ and yaw ψ , are related to the angular momentum of the spacecraft by

$$\phi = \frac{h_z - H_z}{H_n}, \quad \psi = \frac{H_x}{H_n} \quad (4)$$

where h_z is the yaw momentum stored in the wheels and $H_n > 0$ is the momentum bias. Note that the yaw error is proportional to the roll momentum and the roll error is proportional to the net yaw momentum.

For geosynchronous spacecraft, solar torques are the dominant environmental torques. The rotation of the spacecraft bus with respect to the sun causes the solar torques to vary with orbital position. The solar torques acting on a particular spacecraft are estimated by numerical integration of solar pressure over a surface model of the spacecraft at several orbital positions. Then the coefficients of a truncated Fourier series for the resultant roll and yaw torques are calculated, giving

$$T_{dx}(t) = \frac{1}{2}A_{x0} + \sum_{n=1}^{n_{\max}} [A_{xn} \cos(n\omega_o t) + B_{xn} \sin(n\omega_o t)]$$

$$T_{dz}(t) = \frac{1}{2}A_{z0} + \sum_{n=1}^{n_{\max}} [A_{zn} \cos(n\omega_o t) + B_{zn} \sin(n\omega_o t)] \quad (5)$$

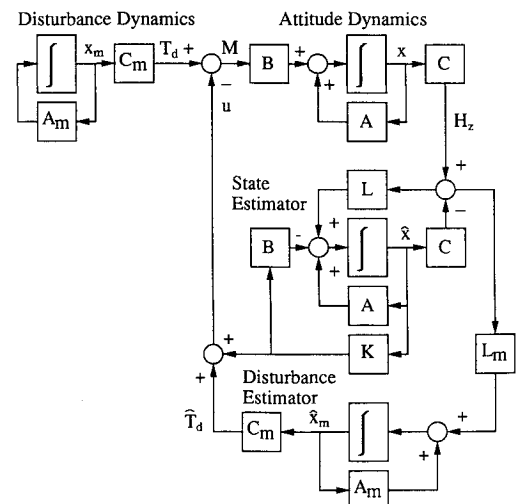


Fig. 1 Control system block diagram.

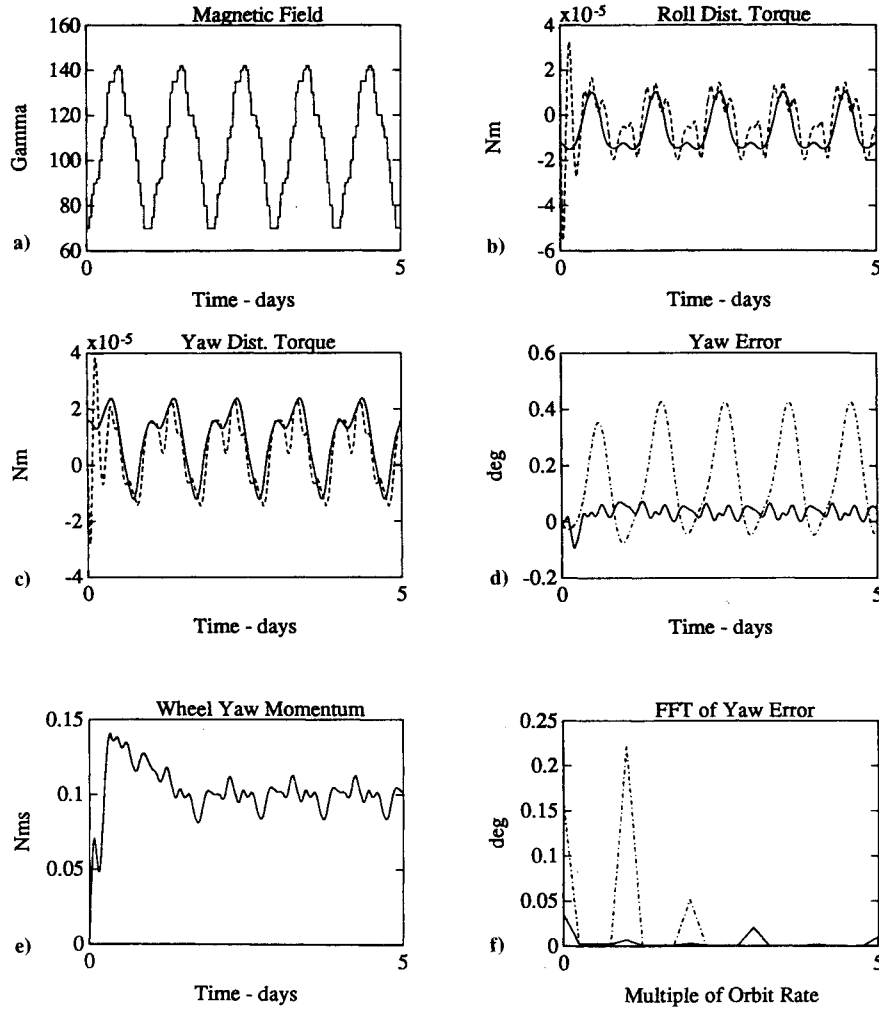


Fig. 2 Five day simulation: a) magnetic field; b) actual (solid) and estimated (dashed) roll disturbance target; c) actual (solid) and estimated (dashed) yaw disturbance torque; d) yaw error with (solid) and without (dash-dotted) disturbance rejection; e) wheel yaw momentum; f) FFT of the yaw response with (solid) and without (dash-dotted) disturbance rejection.

The magnitude ratio R_n and relative phase angle θ_n between the n th harmonic roll and yaw torque vectors are

$$R_n = \sqrt{\frac{A_{xn}^2 + B_{xn}^2}{A_{zn}^2 + B_{zn}^2}}$$

$$\theta_n = \tan^{-1} \left(\frac{B_{zn}}{A_{zn}} \right) - \tan^{-1} \left(\frac{B_{xn}}{A_{xn}} \right) \quad (6)$$

Control System Design

The magnetic torquer control loop stabilizes the long-term response of the orbit rate dynamics and removes the momentum accumulation caused by the environmental disturbance torques. The roll momentum, yaw momentum, and disturbance torques are estimated from the measured yaw momentum and fed through feedback matrices to the roll and yaw magnetic torquers.

Figure 1 shows the control loop block diagram. The spacecraft dynamics are driven by the disturbance torques, $T_d = [T_{dx}, T_{dy}]'$, minus the control torques, $u = [u_x, u_z]'$. The measured output from the dynamics H_z is then fed to a full-order state observer, which generates \hat{x} . Then \hat{x} is multiplied by the feedback matrix K and sent to the roll and yaw magnetic torquers. The error signal $C(x - \hat{x})$ is fed to the disturbance torque observer, which outputs \hat{T}_d . The torque estimates sum

with the state feedback and are sent to the magnetic torquers. The augmented observer matrices are

$$A_a = \begin{bmatrix} A & BC_m \\ 0 & A_m \end{bmatrix}, \quad L_a = \begin{bmatrix} L \\ L_m \end{bmatrix}, \quad C_a = [C \ 0] \quad (7)$$

with the augmented state vector, $x_a = [x, x_m]'$. Chen⁶ showed that the state x , the estimation error $x - \hat{x}$, and the disturbance estimation error $x_m - \hat{x}_m$ converge asymptotically to zero if L_a and K place the poles of $(A_a - L_a C)$ and $(A - BK)$ in the left half of the complex plane.

Observer Design

The first step in the observer design is to choose a disturbance torque model that, when augmented with the spacecraft dynamics, forms an observable system. In Eqs. (5), the disturbance torques are represented as a truncated Fourier series. A model that includes the highest amplitude harmonic of the Fourier series will give the largest reduction in attitude error. The dynamic model for an arbitrary n th harmonic torque has four states: two states for the roll torque output and two for yaw. Depending on the initial conditions, the model can generate any two independent sinusoids with arbitrary magnitude, arbitrary phase, and $n\omega_o$ frequency.

Unfortunately, forming A_a and C_a with a four-state model makes the augmented system unobservable. Physically, certain roll/yaw torques disturb roll momentum but not yaw

Table 1 Simulation parameters

H_n	114.0, N-m-s
ω_o	7.272×10^{-5} , rad/s
ζ	0.7071
ω_n	3.636×10^{-5} , rad/s
R_1	0.8357
R_2	0.7729
θ_1	-90.82, deg
θ_2	-38.93, deg

momentum. Roll and yaw torques with $R_n = n$ and $\theta_n = 90$ deg cause steady-state yaw errors with zero steady-state yaw momentum. Since yaw errors are not sensed, the effects of these torques on the spacecraft attitude are unobservable.

The unobservability of the four-state model requires that a lower-order model be developed. For harmonic output, a two-state model is the only alternative. Using the estimated solar torque coefficients from Eqs. (5), the n th harmonic disturbance torque model is

$$A_m(n) = \begin{bmatrix} 0 & -n\omega_o \\ n\omega_o & 0 \end{bmatrix}, \quad C_m(n) = \begin{bmatrix} A_{xn} & B_{xn} \\ A_{zn} & B_{zn} \end{bmatrix} \quad (8)$$

The number of parameters in this model can be reduced by introducing R_n and θ_n :

$$A_m(n) = \begin{bmatrix} 0 & -n\omega_o \\ n\omega_o & 0 \end{bmatrix}$$

$$C_m(n) = \begin{bmatrix} R_n \cos \theta_n & -R_n \sin \theta_n \\ 1 & 0 \end{bmatrix} \quad (9)$$

The outputs generated by this model have fixed R_n and θ_n . The augmented system is observable as long as $R_n \neq n$ and $\theta_n \neq 90$ deg.

Depending on the size and geometry of a given spacecraft, more than one harmonic may have to be estimated and rejected in order to meet the pointing requirements. The multi-harmonic augmented state matrices are

$$A_a = \begin{bmatrix} A & BC_m(z_1) & \cdots & BC_m(z_r) \\ & A_m(z_1) & & \\ & & \ddots & \\ & & & A_m(z_r) \end{bmatrix}, \quad C_a = [C \ 0 \ \cdots 0] \quad (10)$$

where z_1, \dots, z_r are the r harmonics of the solar torque to be estimated. The observer error dynamics can be stabilized using either pole placement or linear quadratic (LQ) techniques to move the eigenvalues of $(A_a - L_a C_a)$ to the left half plane.

Controller Design

The stability of the spacecraft dynamics is determined by the eigenvalues of $(A - BK)$. The pair (A, B) is controllable from either a roll or a yaw torque. Therefore, in placing the poles of $(A - BK)$, a constraint must be applied to the feedback gains to fix the torque in the roll/yaw plane. Defining

$$K = \begin{bmatrix} K_1 & K_2 \\ K_3 & K_4 \end{bmatrix} \quad (11)$$

and constraining $K_1 = -K_3$ and $K_2 = -K_4$ results in the following gain equations:

$$K_1 = \frac{1}{2\omega_o} (\omega_o^2 + 2\zeta\omega_n\omega_o - \omega_n^2), \quad K_2 = \frac{1}{2\omega_o} (\omega_o^2 - 2\zeta\omega_n\omega_o - \omega_n^2) \quad (12)$$

where ζ and ω_n are the damping ratio and undamped natural frequency of the poles, respectively. These gain equations hold regardless of the number of estimated disturbance torque harmonics. The total feedback signal to the magnetic torquers is equal to the augmented state feedback matrix K_a multiplied by the estimated augmented state vector \hat{x}_a , where

$$K_a = [K \ C_m(z_1) \ \cdots \ C_m(z_r)] \quad (13)$$

Simulation Results

The control system introduced in the previous sections is now applied to a momentum bias spacecraft in geosynchronous orbit. The simulation parameters are summarized in Table 1. The control system rejects the first and second harmonic disturbance torques. The augmented system is observable because $R_n \neq n$ and $\theta_n \neq 90$ deg for $n = 1$ and 2. The simulated dynamics derive from Terasaki.¹ The momentum wheels, nutation dynamics, and nutation controller are included.

Figures 2a-f show the simulated time response of the spacecraft over a period of five days. The magnetic field (Fig. 2a) varies daily with an average value of 107 γ . The actual and estimated roll and yaw disturbance torques, including first through fifth harmonic terms, are plotted in Figs. 2b and 2c. The yaw error (Fig. 2d) is shown with and without disturbance torque estimation. The steady-state yaw error reduces by more than a factor of eight. The wheel yaw momentum (Fig. 2e) is relatively quiet around a bias value of 0.1 N-m-s. Figure 2f shows the frequency components of the yaw error response with and without disturbance torque estimation. The large first and second harmonic responses (dash-dotted line) have been eliminated by the control system (solid line).

Conclusions

This Note has presented a method of designing disturbance rejection control systems for momentum bias spacecraft. Yaw error is not measured and, therefore, not all disturbance torques can be rejected. If the disturbance torques do not have $R_n = n$ and $\theta_n = 90$ deg, then a full-order observer augmented with two states per harmonic of the disturbance torque provides asymptotic disturbance rejection. The simulated response of an example spacecraft demonstrates improved yaw attitude performance by more than a factor of eight.

References

- ¹Terasaki, R. M., "Dual Reaction Wheel Control of Spacecraft Pointing," Symposium on Attitude Stabilization and Control of Dual Spin Spacecraft, U.S. Air Force, El Segundo, CA, CR F04695-67-C-0158, Aug. 1967.
- ²Dougherty, H. J., Scott, E. D., and Rodden, J. J., "Analysis and Design of WHECON—An Attitude Control Concept," AIAA Paper 68-461, AIAA 2nd Communications Satellite Systems Conference, San Francisco, CA, April 1968.
- ³Dahl, P. R., "A Twin Wheel Momentum Bias/Reaction Jet Spacecraft Control System," AIAA Paper 71-951, AIAA Guidance, Control and Flight Mechanics Conference, Hofstra Univ., Hempstead, NY, Aug. 1971.
- ⁴Lebsonck, K. L., "Magnetic Desaturation of a Momentum Bias System," *Journal of Guidance, Control, and Dynamics*, Vol. 6, No. 6, 1983, pp. 477-483.
- ⁵Wie, B., Lehner, J. A., and Plescia, C. T., "Roll/Yaw Control of a Flexible Spacecraft Using Skewed Bias Momentum Wheels," *Journal of Guidance, Control, and Dynamics*, Vol. 8, No. 4, 1985, pp. 447-453.
- ⁶Chen, C., *Linear System Theory and Design*, Holt, Rinehart and Winston, New York, 1984, pp. 504-506.